SUPPLEMENTARY MATERIAL

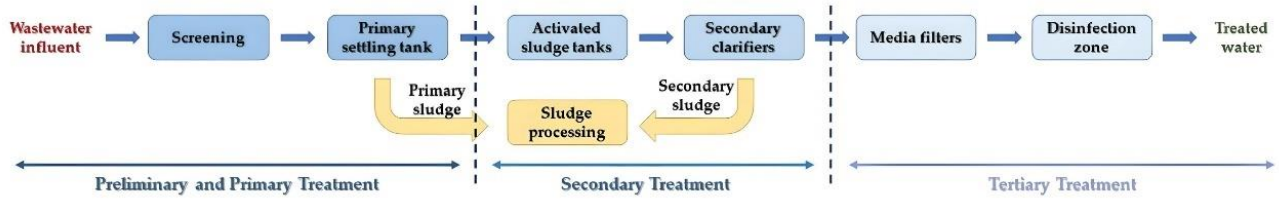

Figure S1. Example of a conventional treatment process in a typical municipal WWTP. Specific unit processes may vary in different MWTPs.

Table S1. d-spacing calculations for commercial TiO_2 (P25) powder.

Bragg's Angle		d_{hkl} (Å)	d_{hkl} (nm)	hkl
2θ	θ			
25.25	12.63	3.5243	0.35243	101 (A)
27.37	13.69	3.2559	0.32559	110 (R)
36.07	18.04	2.4881	0.24881	101 (R)
36.85	18.43	2.4372	0.24372	103 (A)
37.75	18.88	2.3811	0.23811	004 (A)
38.49	19.25	2.3370	0.23370	112 (A)
41.18	20.59	2.1904	0.21904	111 (R)
47.98	23.99	1.8946	0.18946	200 (A)
53.86	26.93	1.7008	0.17008	105 (A)
54.25	27.13	1.6895	0.16895	211 (R)
54.99	27.50	1.6685	0.16685	211 (A)
62.68	31.34	1.4810	0.14810	204 (A)
68.82	34.41	1.3631	0.13631	116 (A)
70.31	35.16	1.3378	0.13378	220 (A)
74.97	37.49	1.2658	0.12658	215 (A)
82.83	41.42	1.1645	0.11645	224 (A)

Table S2. d-spacing calculations for N-doped TiO_2 powder.

Bragg's Angle		dhkl (Å)	dhkl (nm)	hkl
2θ	θ			
25.26	12.63	3.5229	0.35229	101 (A)
27.37	13.69	3.2559	0.32559	110 (R)
37.79	18.90	2.3787	0.23787	004 (A)
48.07	24.04	1.8913	0.18913	200 (A)
53.95	26.98	1.6982	0.16982	105 (A)
54.98	27.49	1.6688	0.16688	211 (A)
62.60	31.30	1.4827	0.14827	204 (A)
68.86	34.43	1.3624	0.13624	116 (A)
70.37	35.19	1.3368	0.13368	220 (A)
75.22	37.61	1.2622	0.12622	215 (A)
82.71	41.36	1.1658	0.11658	224 (A)

Table S3. d-spacing calculations for N,S-codoped TiO_2 powder.

Bragg's Angle		dhkl (Å)	dhkl (nm)	hkl
2θ	θ			
25.27	12.64	3.5215	0.35215	101 (A)
37.71	18.86	2.3835	0.23835	004 (A)
48.03	24.02	1.8927	0.18927	200 (A)
54.61	27.31	1.6792	0.16792	105 (A)
62.73	31.37	1.4800	0.14800	204 (A)
69.21	34.61	1.3564	0.13564	116 (A)
75.20	37.60	1.2625	0.12625	215 (A)
82.77	41.39	1.1652	0.11652	224 (A)

Table S4. d-spacing calculations for Ag@N-doped TiO_2 powder.

Bragg's Angle		dhkl (Å)	dhkl (nm)	hkl
2θ	θ			
25.29	12.65	3.5188	0.35188	101 (A)
37.83	18.92	2.3763	0.23763	004 (A)
44.24	22.12	2.0457	0.20457	200 (Ag)
48.06	24.03	1.8916	0.18916	200 (A)
54.02	27.01	1.6962	0.16962	105 (A)
54.97	27.49	1.6691	0.16691	211 (A)
56.56	28.29	1.6256	0.16256	241 (Ag)
62.64	31.32	1.4819	0.14819	204 (A)
68.94	34.47	1.3610	0.13610	116 (A)
70.31	35.16	1.3378	0.13378	220 (A)
75.18	37.59	1.2628	0.12628	215 (A)
82.82	41.41	1.1646	0.11646	224 (A)

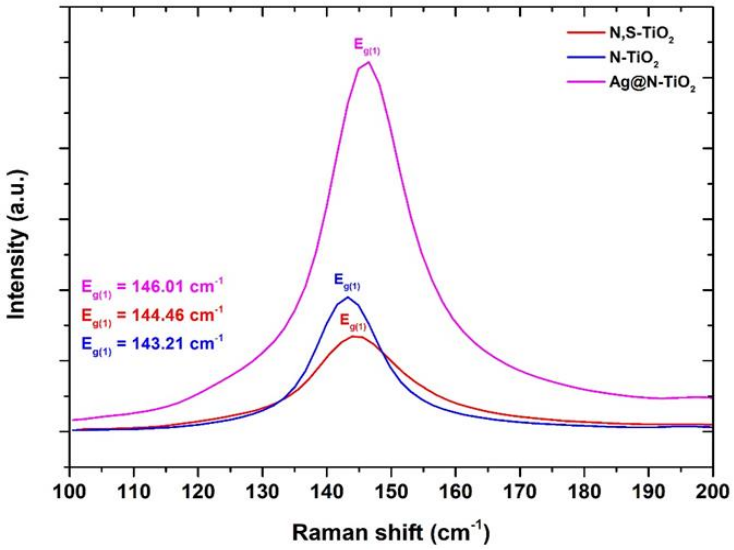

Figure S2. Magnification of $E_{g(1)}$ Raman active mode of anatase TiO_2 phase of the examined chemically modified powders.

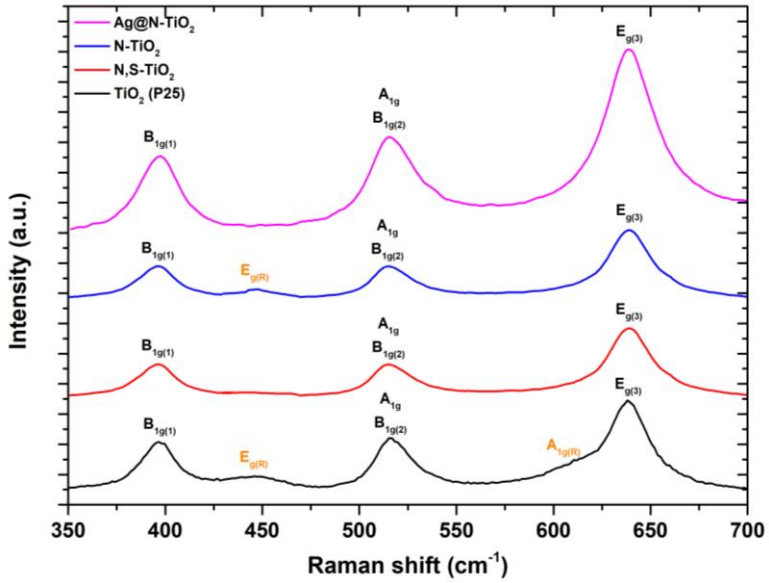

Figure S3. Magnification of 350-700 cm^{-1} Raman spectral region of the studied powders. Anatase TiO_2 modes are marked with black, while rutile TiO_2 modes are marked with orange.

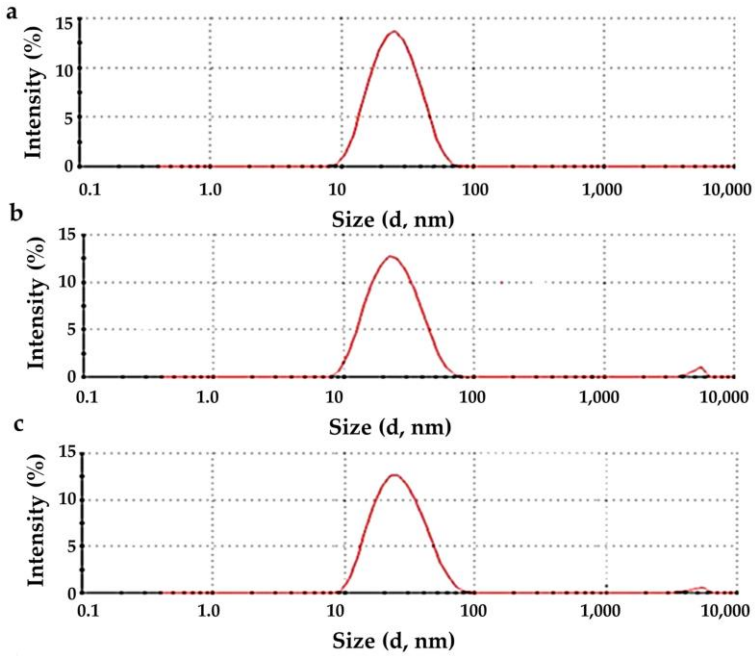

Figure S4. Size distribution diagram of the aqueous dispersion solutions of: (a) Ag@N-TiO_2, (b) N-TiO_2 and (c) N,S-TiO_2 particles.

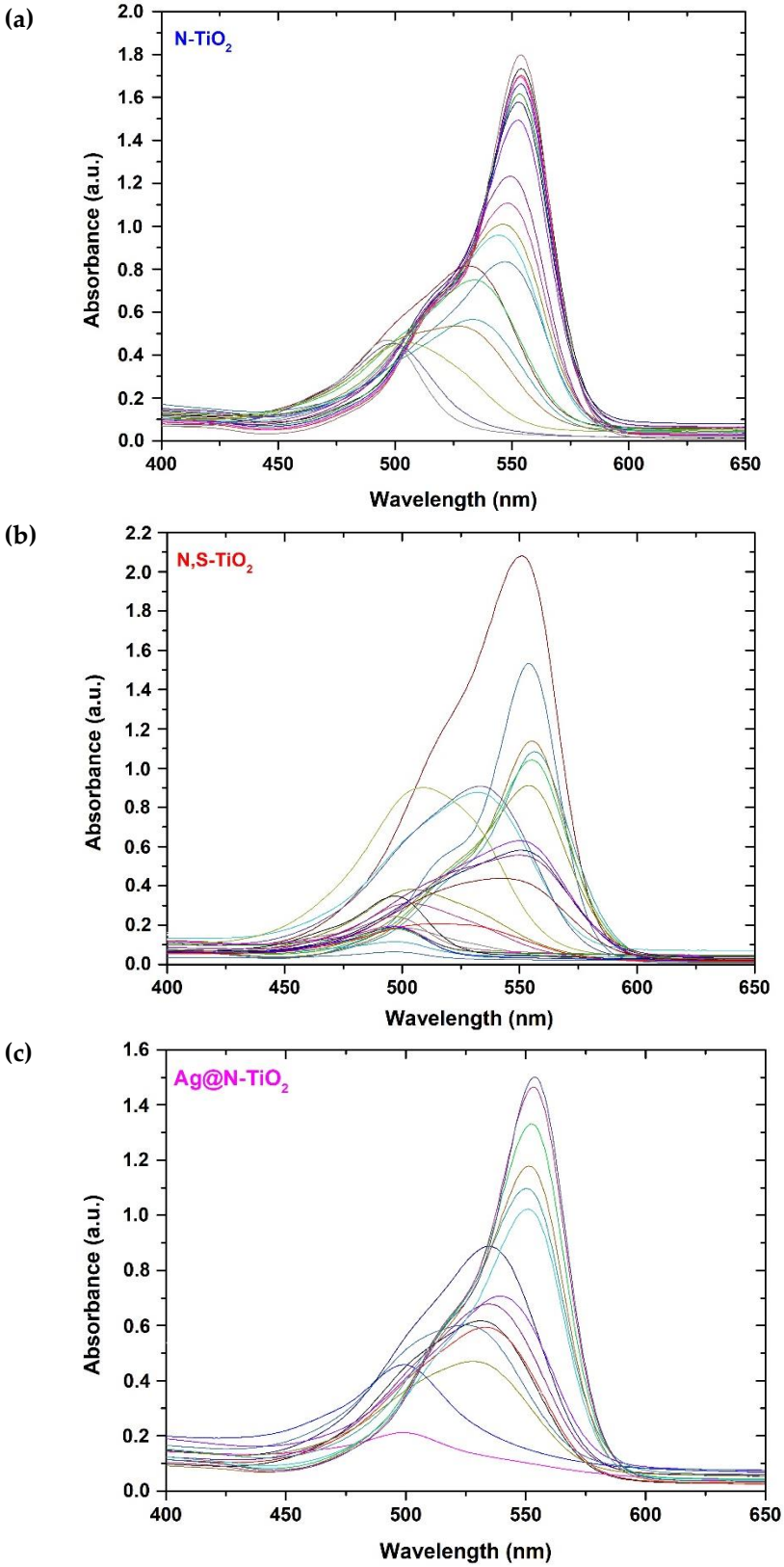

Figure S5. Real time UV-visible spectra obtained every 15 min under visible light photocatalytic degradation of Rhodamine B in presence of: (a) N-doped TiO_2, (b) N,S-codoped TiO_2 and (c) Ag loaded N-doped TiO_2 powder.

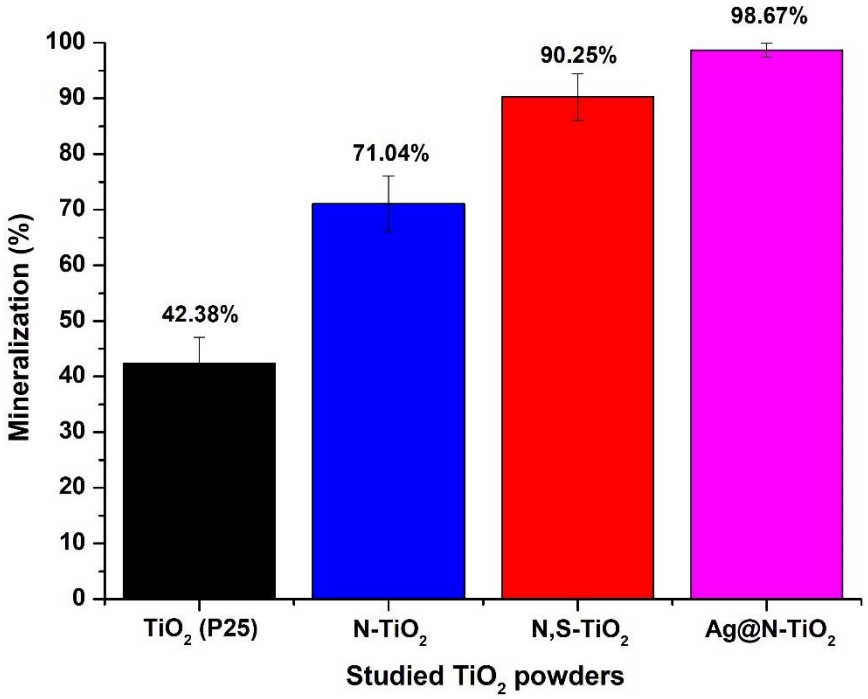

Figure S6. Mineralization (%) of each studied chemically modified TiO_2 sample, obtained through TOC analysis, after the photocatalytic procedure under visible light irradiation.

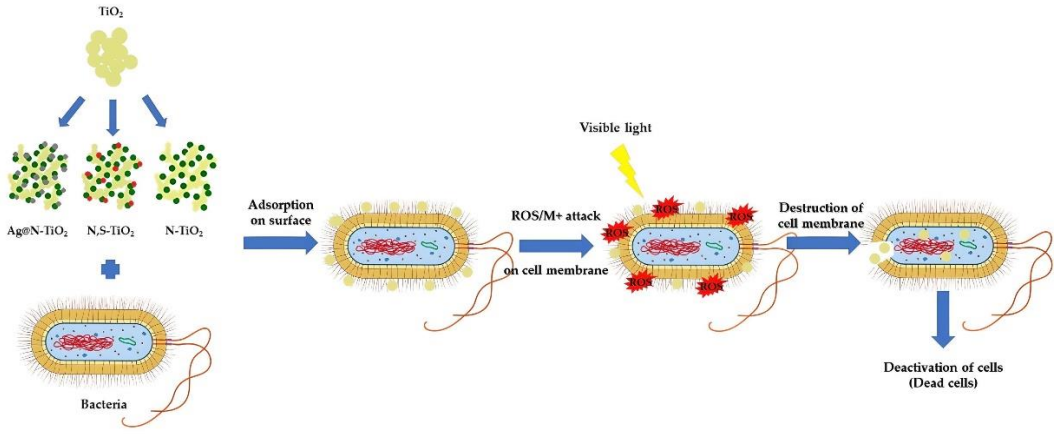

Figure S7. Schematic representation of the photocatalytic disinfection of MWTP effluents containing bacteria using the studied chemically modified TiO_2 powders.

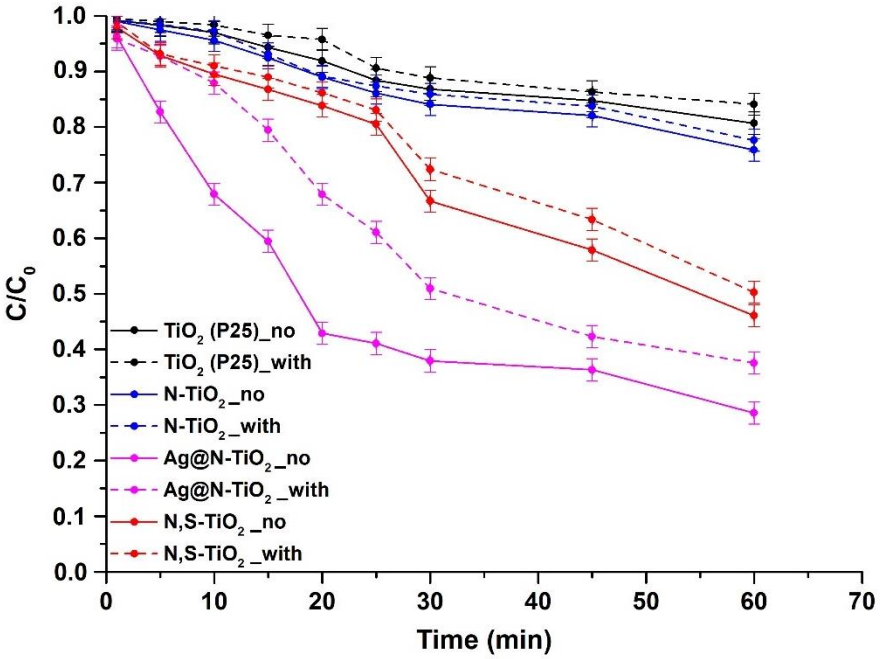

Figure S8. Study of the photocatalytic efficiency of TiO_2 (P25), N-doped TiO_2, N,S-codoped TiO_2 and Ag loaded N-doped TiO_2 powders towards the degradation of RhB dye under visible light irradiation in the presence (dashed line) and in the absence (solid line) of n-butanol •OH scavenger.

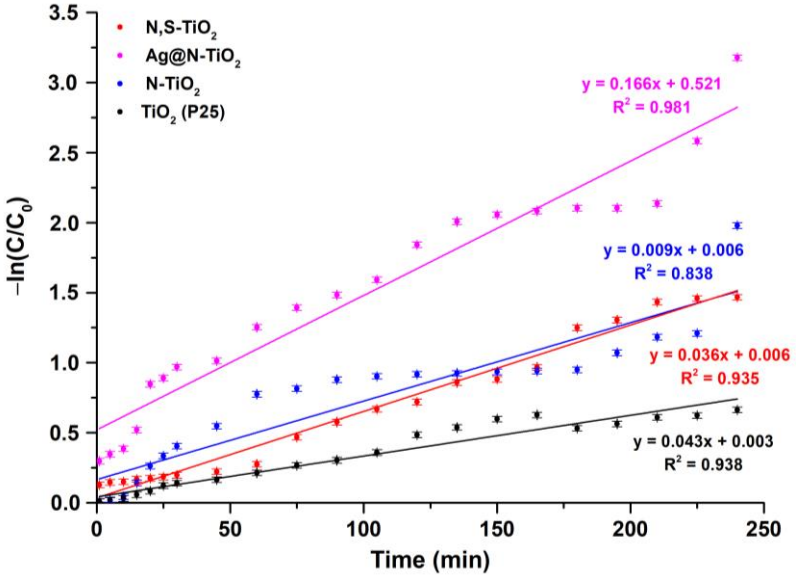

Figure S9. Photocatalytic kinetic model studies for the examined TiO_2 powders following a pseudo-first order model upon visible light irradiation photocatalysis.

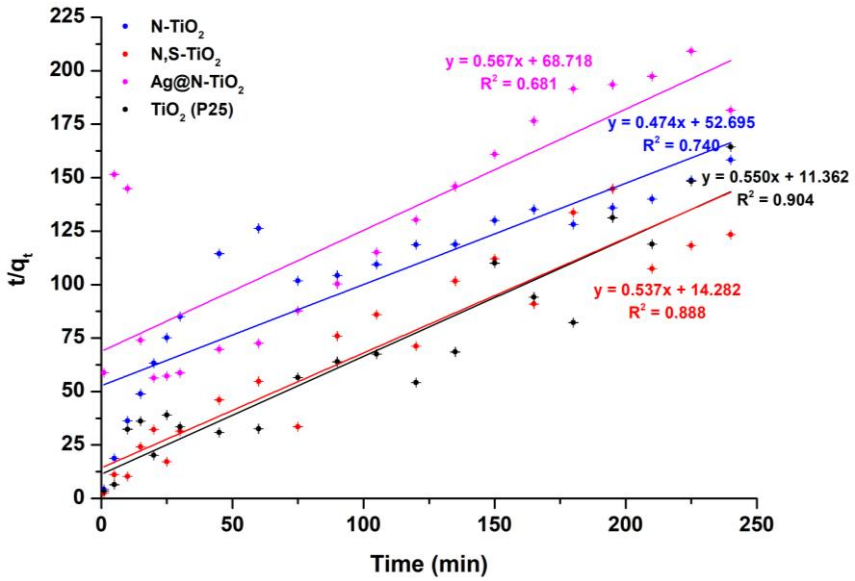

Figure S10. Photocatalytic kinetic model studies for the examined TiO_2 powders following a pseudo-second order model upon visible light irradiation photocatalysis.

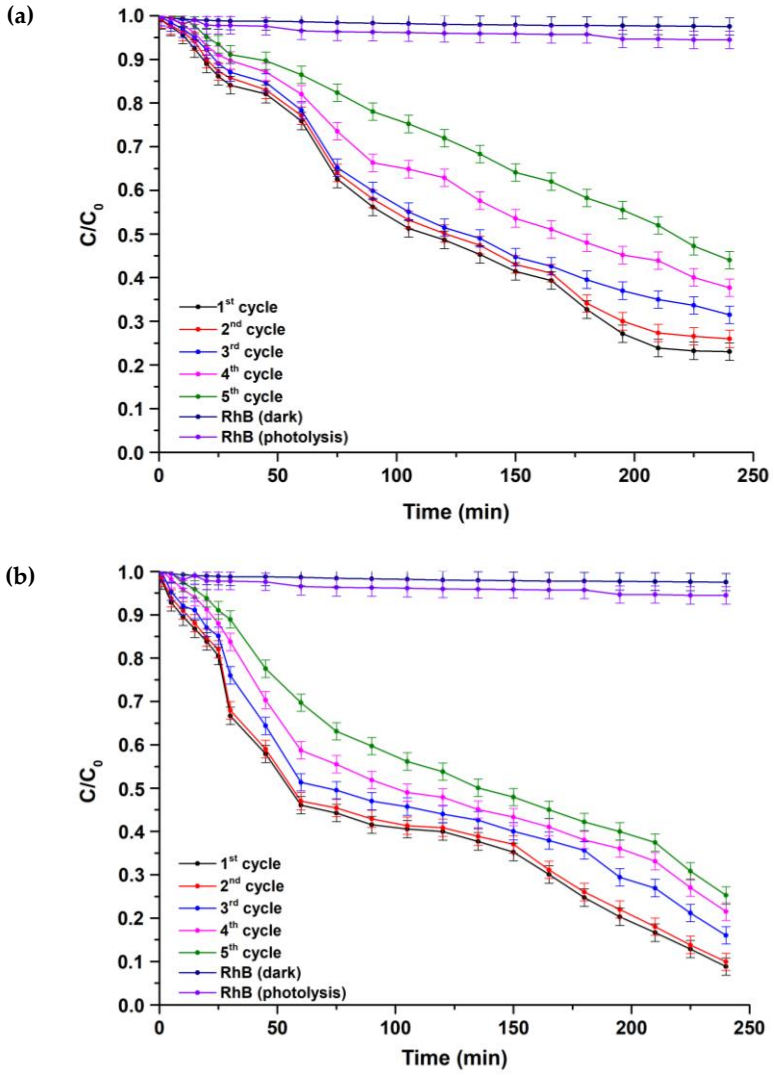

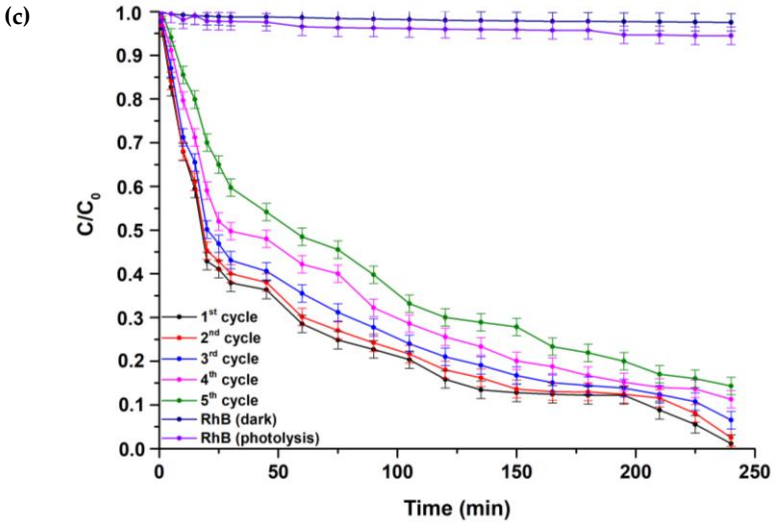

Figure S11. Study of the photocatalytic stability of (a) N-doped TiO_2, (b) N,S-codoped TiO_2 and (c) Ag loaded N-doped TiO_2 powders towards the degradation of RhB dye after 5 cycles under visible light irradiation.

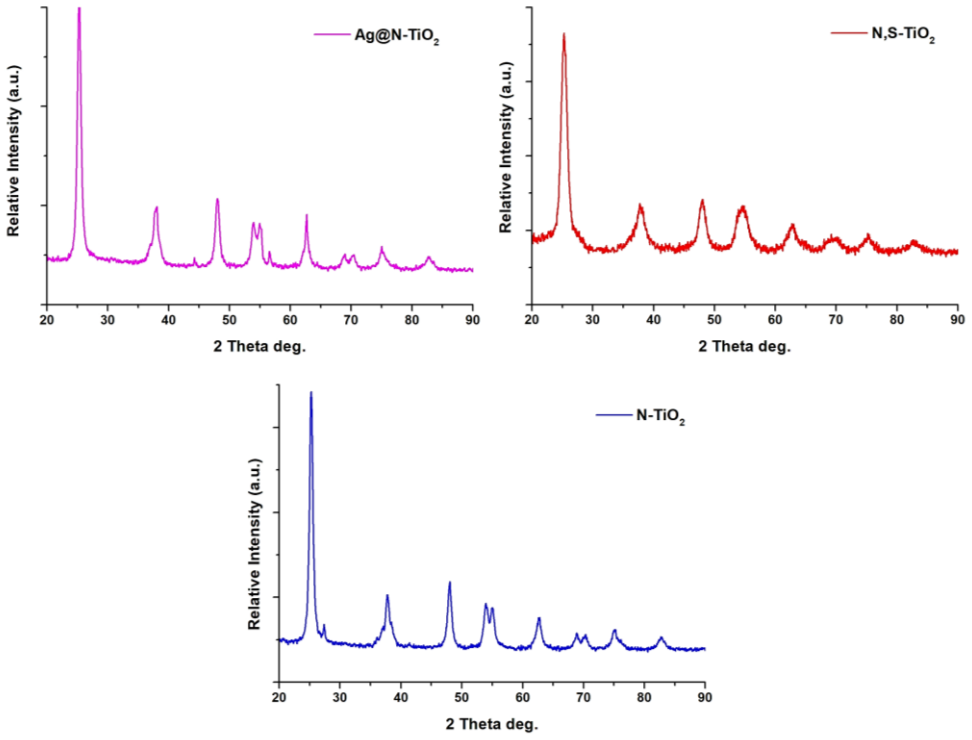

Figure S12. XRD patterns of the studied TiO_2 powders after five photocatalytic cycles of RhB degradation under visible light irradiation.

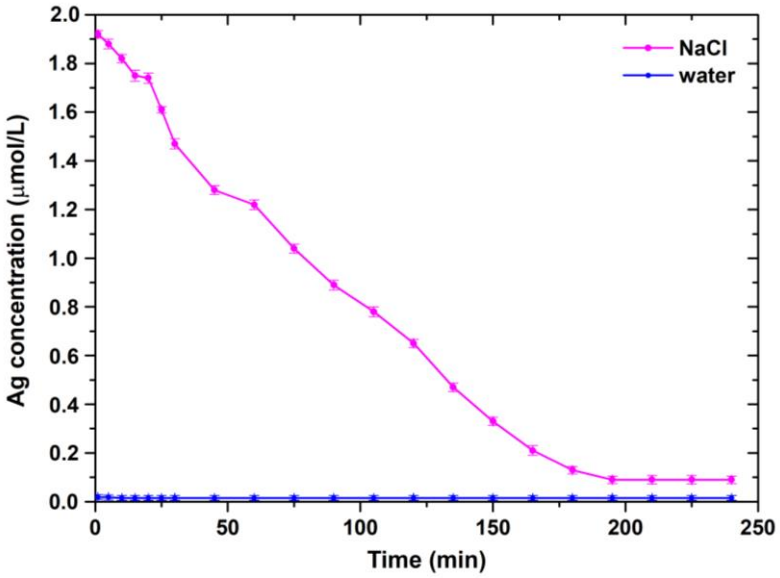

Figure S13. Silver dissolution study for the Ag loaded N-doped TiO_2 powder.